Synthesis of hierarchically structured Fe$_3$C/CNTs composites in FeNC matrix for use as efficient ORR electrocatalysts

Tanlun Wang,[a] Lincheng Xu,[a] Chenxiang Sun,[a] Xiyuan Li,[a] Yong Yan,[b] Fan Li *[a]

a.   Beijing Key Laboratory for Catalysis and Separation, Department of Environment and Chemical Engineering, Beijing University of Technology, Beijing 100124, China.

b.   Beijing Key Laboratory for Catalysis and Separation, Faculty of Environment and Life, Beijing University of Technology, Beijing 100124, China.

*Corresponding author

E-mail: vanadiumli@bjut.edu.cn

Electrochemical measurements

All of the electrochemical measurements were carried with a three-electrode system, including working electrode, reference electrode and counter electrode. The working electrode was chosen by different electrochemical tests. For the cyclic voltammetry (CV) and linear sweep voltammetry (LSV) measurements, a glass carbon working electrode of diameter $\Phi = 4$ mm (area 0.196 cm^2) controlled by the rotating disk electrode (RDE, Pine AFMSRCE). While for rotating ring disk electrode (RRDE, Pine AFMSRCE) measurements, an electrode with a glassy carbon ($\Phi = 5.6$ mm) center and a platinum ring ($\Phi_{outer} = 8$ mm, $\Phi_{inner} = 6.25$ mm) on the outside was used as working electrode. As for chronoamperometry (CA) tests, a glass carbon piece of 10*10 mm was used as working electrode. A Hg/HgO reference electrode (in 0.1 mol/L KOH, 0.165 V vs. RHE) is used as reference electrode and a carbon rod counter electrode ($\Phi = 2$ mm) was used as counter electrode. A customized four-holes flask was used as electrolytic cell, 0.1 mol/L KOH aqueous solution was filled as electrolyte. The electrolyte was saturated in argon firstly to activate the system and then saturated in oxygen for subsequent electrochemical measurements.

The CV and LSV tests were measured with saturated in oxygen 0.1 mol/L KOH aqueous solution at the scan rate of 10 mV/s. For LSV tests, the rotate speed of RDE was in 400, 625, 900, 1225 and 1600 rpm. And the LSV curves of 1600 rpm were chosen for the comparison of ORR activity.

The CA tests were measured at half-wave potential according to the curves of LSV. Oxygen was saturated and continuous during the measured process.

The RRDE test methods were the same as LSV in 1600rpm with the differences in work electrode. The ring current set as 1.4V vs. RHE.

The electrochemical active surface area (ECSA) for each system was estimated from the electrochemical double-layer capacitance (C$_{DL}$) and specific capacitance (C$_S$)[S4, S5]. The value of ECSA is calculated by eq1

$$ECSA = C_{DL}/C_S \qquad\qquad eq1$$

As for C_S, it can be regarded as function of electrolyte system and adopted as 0.04 mF/cm^2 [S6, S7].

Scan rates chose at 10 mV/s, 20 mV/s, 40 mV/s, 60 mV/s and 80 mV/s, ranges are centred on the open circuit potential plus and minus 0.5 V.

The K-L equation can be calculated by eq2:

$$1/J = {}^1\!/_{J_L} + {}^1\!/_{J_K} = 1/B\,\omega^{1/2} + {}^1\!/_{J_K} \qquad\qquad eq2$$

where J is current density at a specific potential, J_L is dynamic current density, J_K is limiting diffusion current density, ω is rotate speed and B is a function of electron transfer number n. A series of plots are described as $(1/J)$-$(1/\omega^{1/2})$ curves with a slope equal to 1/B and the electron transfer numbers n can be calculated. The K-L equation of catalytic material are shown in Figure S8 at the rotate speed of 400, 625, 900, 1225 and 1600 rpm and scan rate of 10 mV/s.

To calculate C_{DL}, the formula was described as eq3:

$$i = v * C_{DL} \qquad\qquad eq3$$

in which i is double-layer current (the current at open circuit potential) and v is scan rate. A series of plots are described as i-v curves with a consequence of linear fitting as shown in Figure 4(b).

Electron transfer number(n) and productivity of hydrogen peroxide are calculated in eq4 and eq5:

$$n = {}^4I_D/(I_D + I_R/N) \qquad\qquad eq4$$

$$\%H_2O_2 = 100 * {}^2I_R/[N(I_D + I_R/N)] \qquad\qquad eq5$$

I_D is current of disk, I_R is current of ring. N is collection coefficient of instrument, which is 0.37 tested by $K_3Fe(CN)_6$ solution.
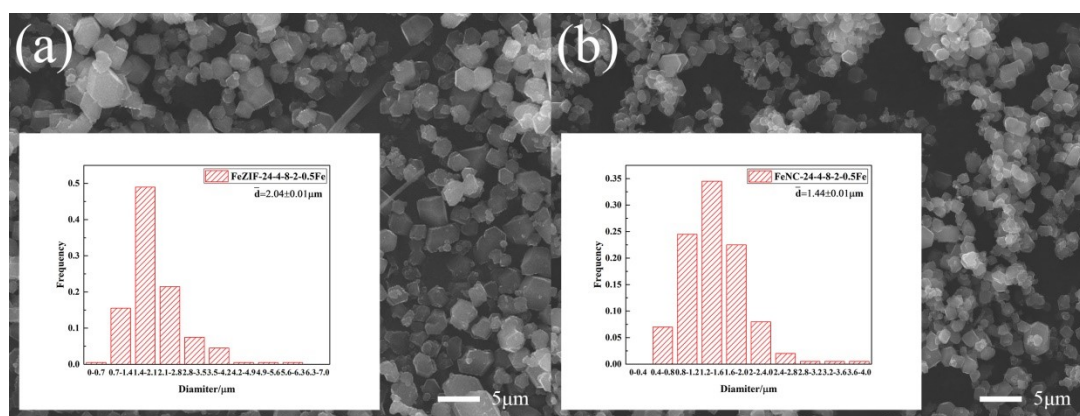

Figure S1. The SEM image and size distribution statistics of FeZIF-2-0.5Fe(a), FeNC-2-0.5Fe(b), FeZIF-32(c) and FeZIF-36(d)
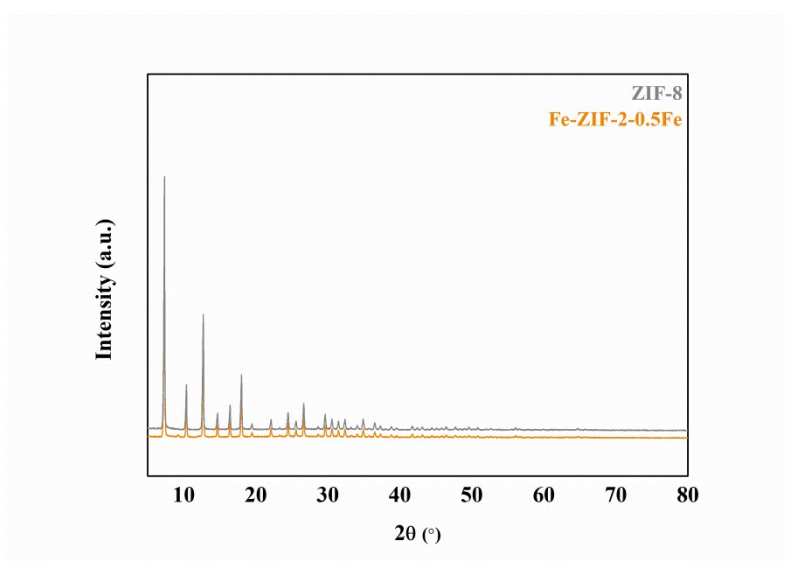
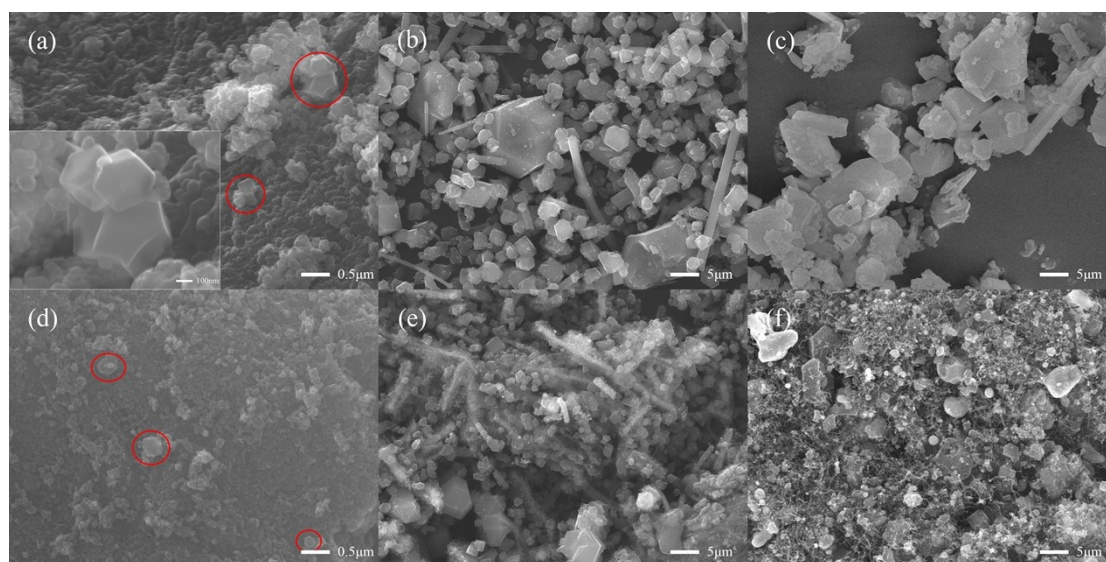Figure S2. The XRD pattern of FeZIF-2-0.5Fe and ZIF-8

Figure S3. The SEM image of (a) FeZIF-2-NO$_3$, (b) FeZIF-2-Ac, (c) FeZIF-1-Ac; (d) FeNC-2-NO$_3$, (e) FeNC-2-Ac, (f) FeNC-1-Ac
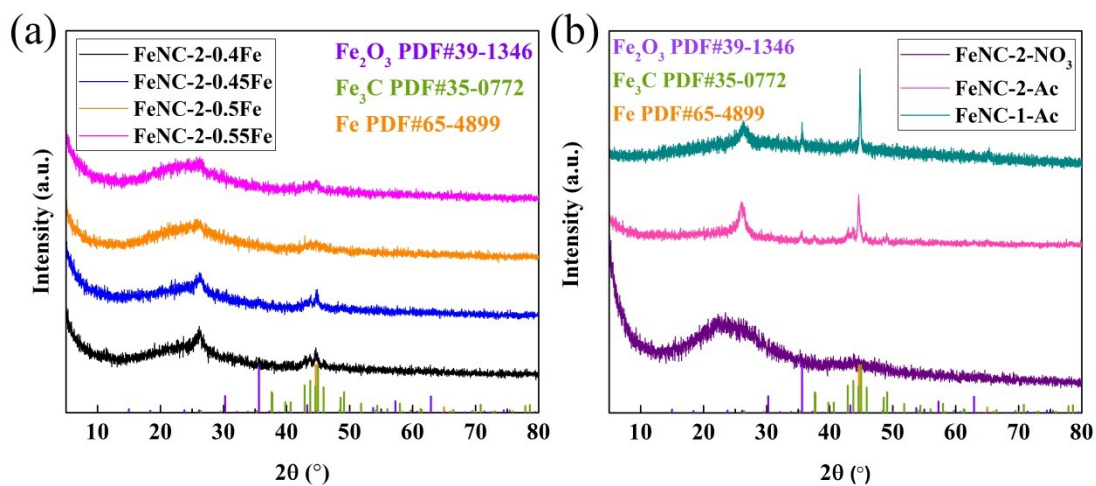
Figure S4. The XRD pattern of (a) FeNC-2-0.4Fe, 0.45Fe, 0.5Fe and 0.55Fe; (b) FeNC-2-NO$_3$, Ac and FeNC-1-Ac
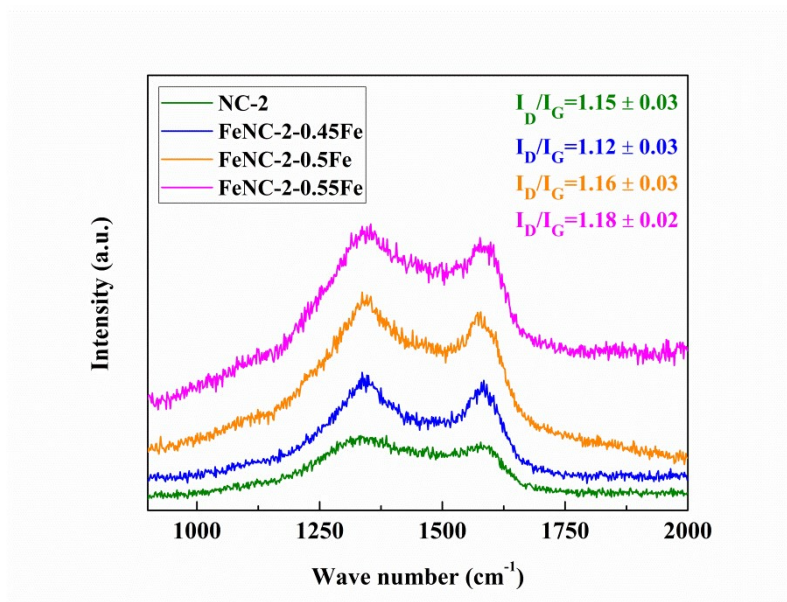

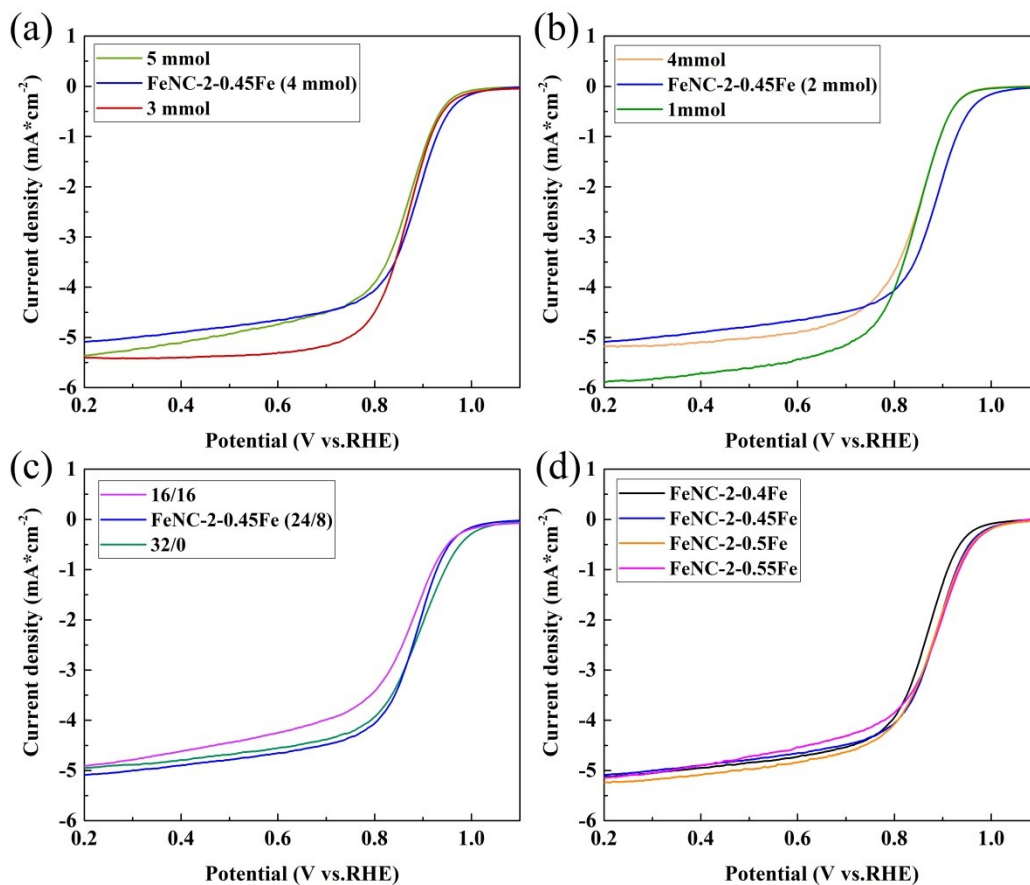Figure S5. The Raman spectroscopy results of FeNC-2-0.45Fe, 0.5Fe, 0.55Fe and NC-2

Figure S6. The LSV curves of catalysts in different synthesis conditions (a) the dosage of $Zn(Ac)_2$, (b) the dosage of $Zn(NO_3)_2$, (c) the dosage of HMIM in two steps, (d) the dosage of Fe
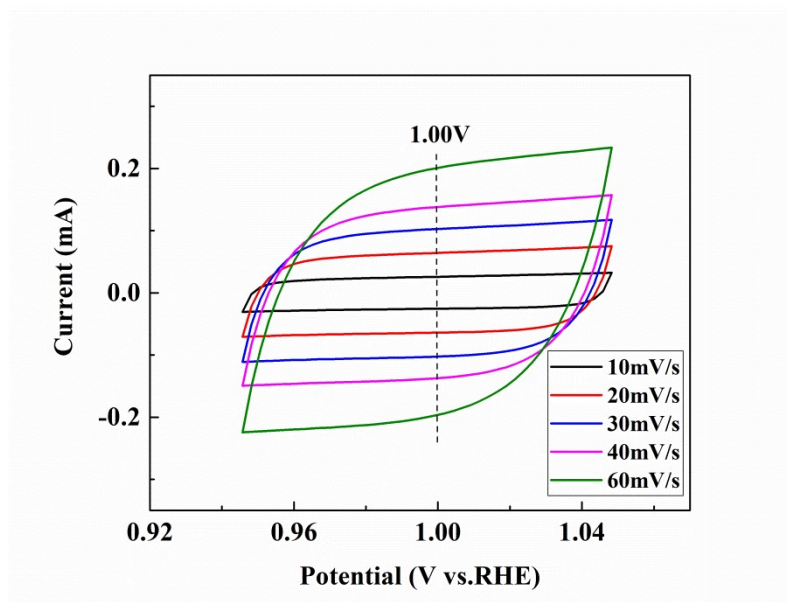

Figure S7. The CV curves of FeNC-2-0.5Fe in non-Faradaic region, scan rates are 10 mV/s, 20 mV/s, 30 mV/s, 40 mV/s, 60 mV/s
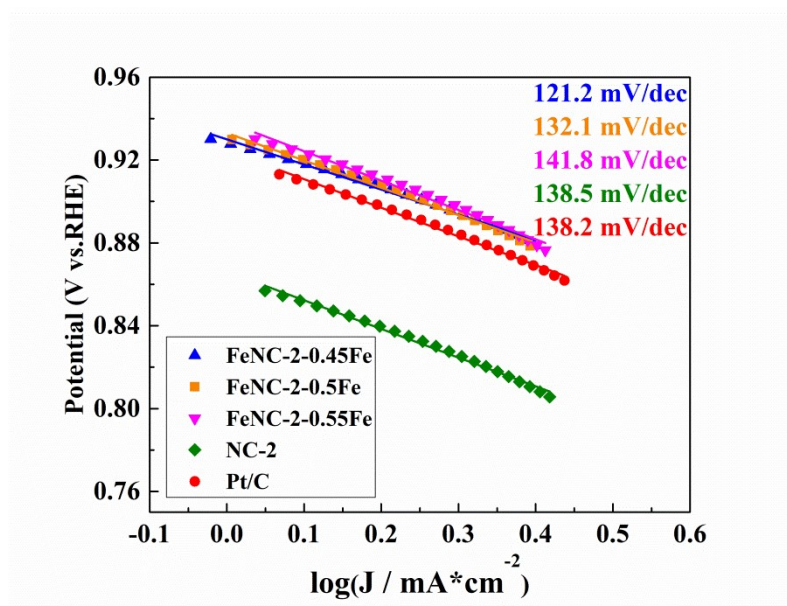
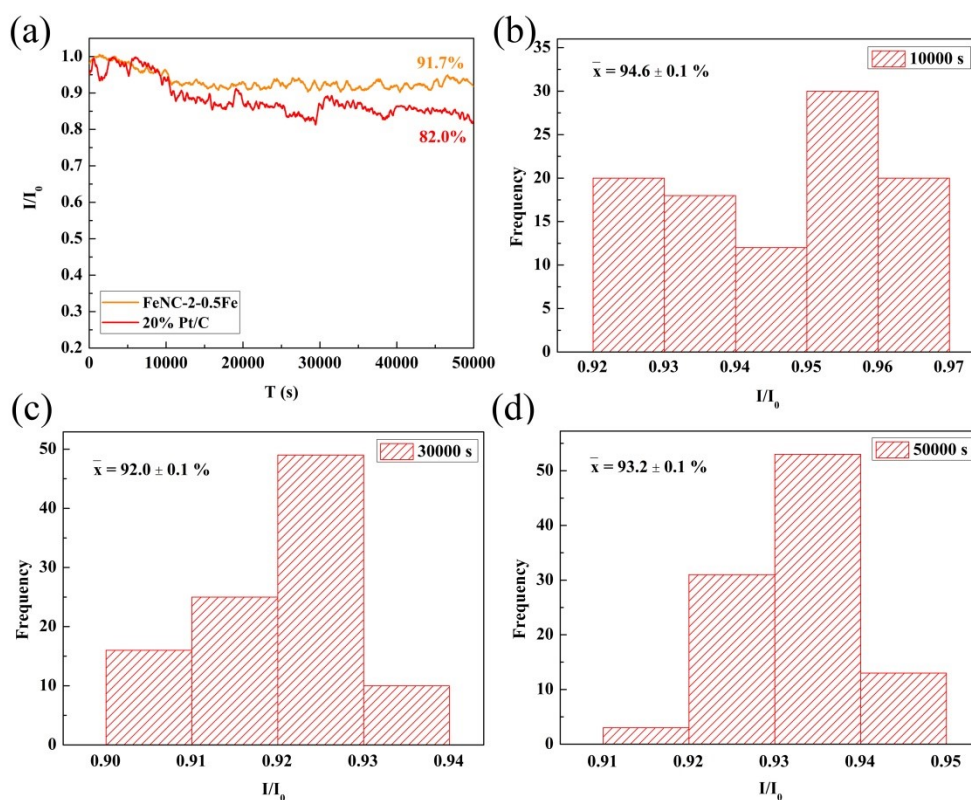Figure S8. The Tafel plots of FeNC-2-0.45Fe, 0.5Fe, 0.55Fe, NC-2 and Pt/C

Figure S9. The CA curves of FeNC-2-0.5Fe and Pt/C (a) and the histogram of 100 points selected within ± 3000 s
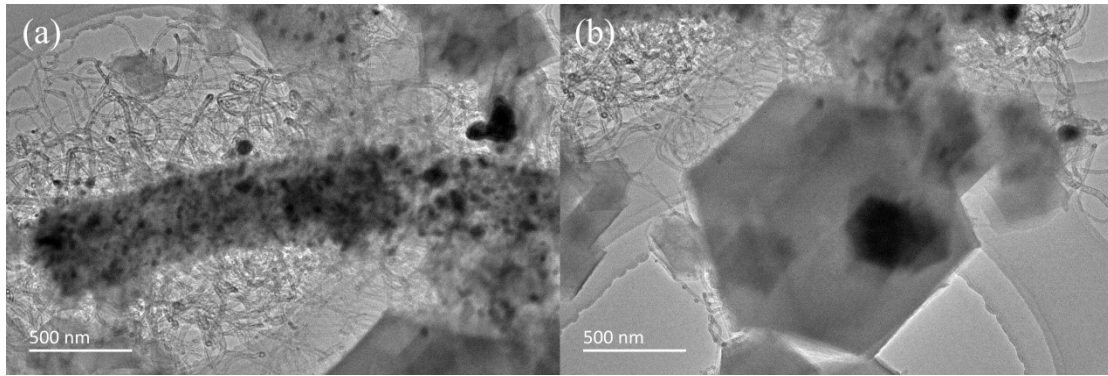
of 10000 s (b), 30000 s (c) and 50000 s (d)

Figure S10. The TEM images of FeNC-2-0.5Fe after CA test. (a) rod-like structure, (b) ZIF-like carbon

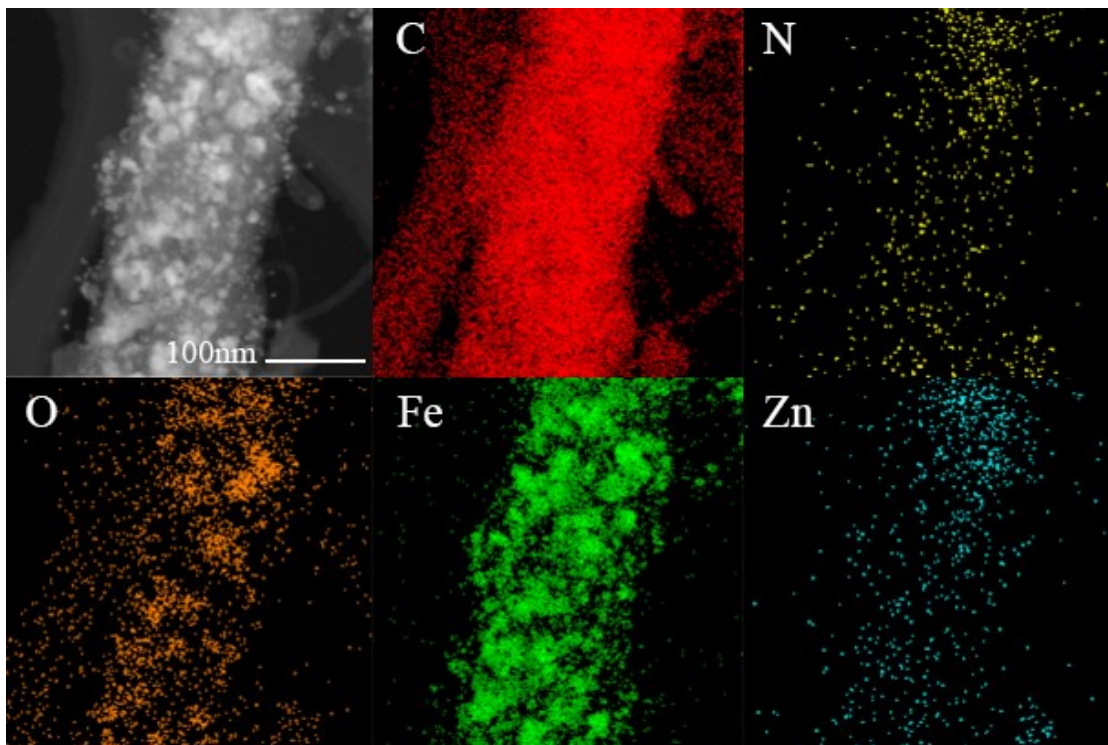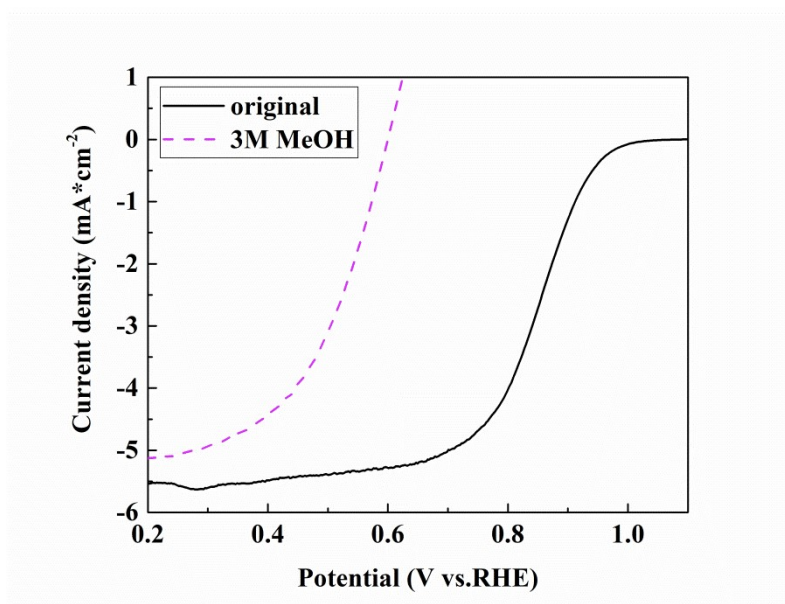Figure S11. The EDS-mapping of FeNC-2-0.5Fe after CA test

Figure S12. LSV curves of Pt/C in 0.1 M O_2-saturated KOH solution in 1600 rpm with methanol at 3.0 M

Table S1. The atomic ratio of Fe measured by XPS and ICP-OES

Name of sample	The ratio of Fe atom (%)	
	XPS	ICP-OES
FeNC-2-0.45Fe	0.39	0.85
FeNC-2-0.5Fe	0.56	1.50
FeNC-2-0.55Fe	0.37	1.21

Table S2. Comparison of ORR catalytic performance for benchmark Pt/C and M-NC based catalysts

Catalysts	Electrolyte	Half-wave potential for ORR (V vs .RHE)	Limiting diffusion current density (mA cm^{-2})	Ref.
Pt/C	0.1 M KOH	0.861	~ -5.50	This work
Fe-2-WNPC-NCNTs	0.1 M KOH	0.84	~ -5.41	5
FCTN@CNTs	0.1 M KOH	0.95	~ -5.55	6
FeMn@BNPCFs-900	0.1 M KOH	0.868	~ -6.21	7
Fe-Fe$_3$C-NCT	0.1 M KOH	0.851	~ -8.05	8
Fe/Fe3C-0.6-NP@NC	0.1 M KOH	0.85	~ -5.69	9
Fe-CZIF-800-10	0.1 M KOH	0.821	~ -5.83	10
1MIL/40ZIF-1000	1.0 M KOH	0.88	~ -4.75	11
Fe/N-HCNFs	0.1 M KOH	0.834	~ -6.53	12
FeNCFs	0.1 M KOH	0.84	~ -5.70	13
hollow Fe$_3$C/N-rGO	0.1 M KOH	0.829	~ -5.42	14
Our work	0.1 M KOH	0.878	~ -5.23	--

References

S1   S. Trasatti, O. Petrii, *Pure Appl. Chem*., 1991, **63**, 711-734.

S2   C. C. McCrory, S. Jung, J. C. Peters, T. F. Jaramillo, *J Am Chem Soc.*, 2013，**135**, 16977-16987.

S3   R. Ma, G. Lin, Q. Ju, W. Tang, G. Chen, Z. Chen, Q. Liu, M. Yang, Y. Liu, J. Wang, *Appl. Catal., B,* 2020, **265**, 118593.

S4   C. Shao, S. Zhuang, H. Zhang, Q. Jiang, X. Xu, J. Ye, B. Li, X. Wang, *Small*., 2021, **17**, 2006178.

S5   Z. Liu, Y. Zhu, K. Xiao, Y. Xu, Y. Peng, J. Liu, X. Chen, *ACS Appl. Mater. Interfaces*., 2021, **13**, 24710-24722.

S6   K. Li, C. Wang, H. Li, Y. Wen, F. Wang, Q. Xue, Z. Huang, C. Fu, *ACS Appl. Mater. Interfaces*., 2021, **13**, 47440-47448.

S7   Z. Liu, F. Guo, L. Han, J. Xiao, X. Zeng, C. Zhang, P. Dong, M. Li, Y. Zhang, *ACS Appl. Mater. Interfaces*., 2022, **14**, 13280–13294.

S8   Y. Wang, L. Wang, Y. Xie, M. Tong, C. Tian, H. Fu, *ACS Sustainable Chem. Eng.*, 2022, **10**, 3346-3354.

S9   L. Luo, Y. Xu, D. Wang, W. Feng, X. Qiu, *Inorg. Chem.*, 2022, **61**, 3166-3175.

S10 G. Li, J. Zhang, W. Li, K. Fan, C. Xu, *Nanoscale*., 2018, **10**, 9252-9260.

S11 H. Wang, F. Yin, N. Liu, R. Kou, X. He, C. Sun, B. Chen, D. Liu, H. Q. Yin, *Adv. Funct. Mater.,* 2019, **29**, 1901531.

S12 Q. Li, J. Zhao, M. Wu, C. Li, L. Han, R. Liu, *ChemistrySelect*., 2019, **4**, 722-728.

S13 Y. Ma, D. Chen, D. Zhang, H. Yu, Y. Zheng, W. Li, L. Wang, Q. Liu, W. Yang, *Carbon*, 2022, **187**, 196-206.

S14 Y. Wang, N. Wu, Y. Qi, Z. Zhu, T. Zhang, X. Han, S. Li, J. Wu, J. Qiu, *Appl. Surf. Sci.*, 2022, **585**, 152569.